

## A NOVEL TRIAXIAL APPARATUS TO EVALUATE THE EFFECT OF HIGH TEMPERATURE NITROGEN INJECTION Concept and Design

by

**Sheng-Cheng WANG<sup>a\*</sup>, Ya-Nan GAO<sup>b</sup>, Lan-Ying HUANG<sup>a</sup>,  
Hai-Jian LI<sup>c</sup>, and Shan-Jie SU<sup>a</sup>**

<sup>a</sup> School of Civil Engineering, Xuzhou University of Technology, Xuzhou, China

<sup>b</sup> State Key Laboratory for Geomechanics and Deep Underground Engineering,  
China University of Mining and Technology, Xuzhou, China

<sup>c</sup> College of Geology and Mines Engineering, Xinjiang University, Urumqi, China

Original scientific paper

<https://doi.org/10.2298/TSCI2106527W>

*High temperature nitrogen injection into coal seams is supposed to improve the permeability and thus maintain the safety of underground mining. A novel triaxial apparatus is recently developed, aiming at providing the effective method to evaluate the effect of high temperature nitrogen injection. The main feature of this novel apparatus is its high confining pressure, gas injection with high pressure as well as the high temperature. This new device can be either used for natural coal samples (e.g. intact or fractured) or the synthetic coal samples. A series of leakage tests were conducted to verify the feasibility of this instrument, the results of which have confirmed that the maximum pressure (i.e. 10 MPa) can be reached. In addition, the high temperature and pressure of nitrogen gas can also be sustain at the requested level. Based on the preliminary tests on the instrument, a large amount of tests were carried out to evaluate the effect of nitrogen injection in enhancing the permeability of coking coal from the Pingdingshan coalfield, China, and the influence of high temperature nitrogen injection on mechanical parameters of coal was obtained.*

Key words: triaxial test, nitrogen injection, high temperature, high pressure, low permeability

### Introduction

Coal is main energy of China, which takes up more than 70% of Chinese primary energy production and consumption structure [1-3]. Among them, more than 70% of the coal seams' permeability is lower than 1 mD [4]. With the depletion of shallow coal resources, the mining depth has found the quickly increasing during the past decades [5]. Correspondingly, the gas pressure and its content in coal seams become larger than that in shallow mining. As a result, a large amount of mine accidents related to gas emission in these coal seams with low permeability were reported, which has drawn much attention either from the coal operators or the researchers around the world [6, 7]. There are different technical methods widely applied to improve the coal permeability in coal mines, including the hydraulic fracturing, CO<sub>2</sub> injection, and N<sub>2</sub> injection.

As a new technology, high temperature N<sub>2</sub> injection into coal seams has been proposed. It is expected that the injection of N<sub>2</sub> into coal seams can improve the coal permeability

\* Corresponding author, e-mail: scwang@xzit.edu.cn

better and expand the gas extraction area. Even though, the complex geological conditions and specific mining methods make it difficult to investigate the effect of  $N_2$  injection with temperature and pressure on permeability of low permeability coal by these onsite case studies. Different from the trial tests conducted onsite, the laboratory tests are generally regarded as one of the most effective methods.

It has been well noted that both the stress and gas pressure at different mining depths are different from each other and the importance of triaxial testing is thus much obvious. To date triaxial tests are widely used in geomechanics engineering to investigate the mechanical and permeability behavior of coals under different confining stresses [8]. There are also lots of related studies conducted to investigate the coupled behavior of fluid (*e.g.*  $CO_2$ ,  $CH_4$ ,  $N_2$ ) migration and to further examine their flow and strength behavior [9-13]. Barla *et al.* [14] introduced a new triaxial equipment capable of investigating mechanical properties of rock at confining pressures up to 64 MPa. To the best knowledges of the authors, existing triaxial test apparatus are generally designed for normal use, which is not capable to capture the mechanical behavior of coal seams treated with the  $N_2$  injection.

This paper introduces a novel triaxial apparatus developed and housed at China University of Mining and Technology, China. The most attractive features of this apparatus is its high confining pressure, injection pressure and elevated temperature ( $N_2$  and coal). The design caters for experimental simulation studies of mechanical a behavior during  $N_2$  injection and has the capacity to simulate the range of stresses, injection pressures and temperatures expected for improve coal permeability.

The new triaxial equipment can be used to conduct permeability and strength tests for 50 mm diameter cylindrical samples consisting of rock (*i.e.* coal, sandstone, and mudstone) or synthetic materials analogous to rock (*i.e.* cement, reconstituted coal). Samples can be intact or fractured. Tests can be carried out at confining pressures up to 80 MPa to simulate ground pressures to depths in excess of 2.2 km. However, there is a temperature limit of 60 °C and temperature at such depth of 2.2 km could exceed 60 °C depending on geological condition. The  $N_2$  gas injection can be carried out at pressures up to 25 MPa and temperature up to 120 °C.

### Novel triaxial apparatus

To evaluate the effects of high temperature  $N_2$  injection for coal samples with low permeability, there are two critical parameters (*i.e.* temperature and pressure) to be accounted for in the laboratory test. As depicted in fig. 1, the novel triaxial apparatus consists of the following four components:

- servo loading system,
- heating systems (for  $N_2$  or/and coal heating),
- gas injection system, and
- data measurement system.

Some critical data including the lateral stress, lateral displacement, axial stress, axial displacement, fluid injection and outlet flow rates can be simultaneously recorded by a data logger embedded in the data measurement system.

#### *Servo loading system*

The servo load system is the most important component of the designed instrument, which can apply the axial load and lateral loading on the tested coal sample. The servo loading system mainly relies on the operation of the main pumps and screw joint load (holding pressure part). As shown in fig. 1, the host, force sensors, displacement sensors and servo hydraulic parts

are fixed together to provide the axial load with the maximum force of 2000 kN. The measurement resolution is 1/180000, associated with the effective ranging from 2-2000 kN. The test force, displacement, distortion of the control fluctuation are smaller than  $\pm 1/2500$ ,  $\pm 1/5000$ ,  $\pm 1/2500$ , respectively. Axial control includes test force, displacement, deformation (axial and radial), and the three control modes can be no impact on conversion. Loading rate: test force is 0.01- 100 kN per second, displacement is 0.005-10 mm per minute, distortion is 0.001-1 mm per minute.

Lateral loading system includes the self-balancing triaxial pressure chamber, pressure sensors, EDC monitoring and a pressure device. The maximum confining pressure provided by the chamber is 80 MPa (60 MPa under high temperature) with a measurement accuracy of 0.5%. Note that the confining pressure resolution of the lateral loading system is 1/180000, while the control fluctuation is 1/5000. The pressurized rate of this lateral loading system ranges from 0.01-0.5 MPa per second.

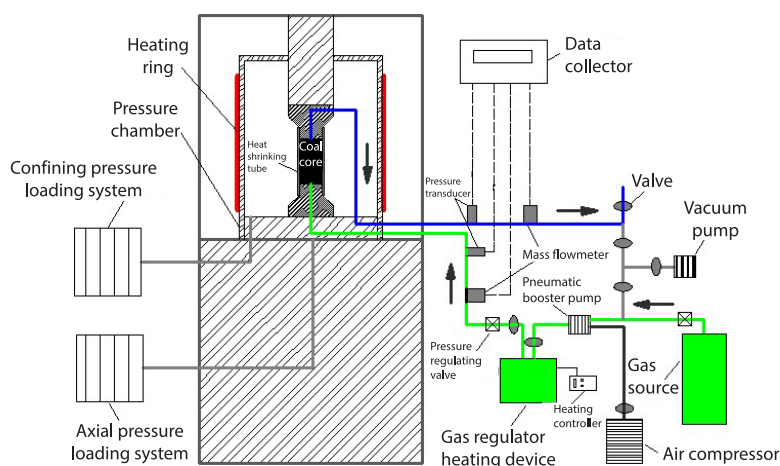


Figure 1. Schematic of the experimental system

### Heating system

The heating system is a unique feature of this triaxial set up and was specially added to ensure that injected  $N_2$  remains in a state during migration through the coal sample and analog ground temperature. The heating system consists of two parts, which are the heating portion of the coal samples and gas. In practices, the coal sample is heated by the heating ring, and the gas is heated by  $N_2$  special heater. Parameters of temperature control system are shown in tab. 1. The heating ring can be used to achieve operating temperatures up to 60 °C and can therefore, be used to investigate the in-situ temperature effect on gas migration through coal masses. The heating ring comprises a 500 mm diameter, 150 mm height heating blanket that is used to heat the pressure chamber and consequently the coal sample. The  $N_2$  special heater can heat  $N_2$  to a given temperature as designed.

Table 1. Parameters of temperature control system

Coal heating section	Temperature range	Room temperature –60 °C
	Fluctuation	$\pm 1$ °C
	Temperature gradient	1/80 °C
$N_2$ heating section	Temperature range	Room temperature –120 °C
	Fluctuation	$\pm 1$ °C
	Temperature gradient	1/80 °C
	The maximum gas pressure	25 MPa

### *Gas injection system*

Gas injection system includes the gas booster and the heating section. Low pressure  $N_2$  provided by the gas bottle is pressurized by pneumatic booster pump, then injected into the gas regulator heating device. Heating controller maintains the  $N_2$  temperature. After adjustment of the pressure regulating value,  $N_2$  meets of the test requirements. The high temperature  $N_2$  is injected into coal sample. The gas injection system can be used to achieve operating pressure up to 25 MPa. To ensure the safety of gas injection, we installed check valves to protect the gas bottle from back flow in the system.

### *Data measurement system*

The EDC's all-digital servo monitoring device imported from DOLI company, Germany is applied to be the main content of the controlling system. The monitoring device has multiple measurement channels controlled individually. Note that these channels can be no impact conversion in the test. The monitoring device is easy to operate, fault-tolerant, accurate measurement, protection function, high accuracy control. However, all tested data can be automatically collected and recorded on time. The data measurement system consists of deformation measurement device, pressure transducers, flow transducer, displacement transducers and the temperature probe, which will be outlined in:

- *Deformation measurement device*: the force-deformation of the coal sample is converted into an electrical signal using deformation sensors via varistor and the signal data processing. Then the actual value of deformation is recorded in the database of the file system. The measurements of axial and radial sensor are the mean values of four fulcrums, and this measurement method can ensure the accuracy of the measurement.
- *Pressure transducers*: pressure transducers are used to monitor the axial pressure, confining pressure and  $N_2$  injection pressure. For the set-up, YPR-10 type pressure transducers are used to measure the confining pressure inside the cell, LTR-2 type pressure transducers are used to measure the axial pressure, and gas injection pressures to the bottom of the sample. The pressure transducers used to measure the confining pressure ranging from 0-120 MPa and the large range of axial pressure (*i.e.* 0-2000 kN). Whereas, these gas transducers are capable of measuring pressures up to 25 MPa, which is about twice the nominal pressure.
- *Flow transducer*: the flow transducer of D07 type is adopted to monitor the outlet flow which is the most critical part of coal permeability measurements as stated in Darcy's law. The flow transducer can measure from 0-999.9 ml per minute with a  $\pm 2.5\%$  accuracy. This flow transducer can be used to record the pressure (*i.e.* 0-10 MPa) and the temperature (*i.e.* 20-120 °C).
- *Displacement transducers*: the triaxial equipment is fitted with two displacement transducers to measure the axial and radial displacements. One DC to DC linear variable differential transformer (LVDT) type displacement transducers (with captive guided option) are mounted on the loading ram (above the pressure cell) to measure the axial displacement. One strain gauge attached clip gauges are placed on the sample to measure the radial displacement. The stainless steel LVDT, with a range of  $\pm 30$  mm, carry an accuracy of measurement of  $\pm 0.25\%$  of full scale of linearity. The displacement transducers are capable of operating at a variety of temperatures, from 0-100 °C.
- *Temperature probe*: the PT100 type temperature probes are used to measure temperature inside the pressure chamber and gas regulator heating device. The size of the temperature probe was decided with consideration of the limited space available inside the cell. The temperature prober can measure from  $-50$ -300 °C with a  $\pm 1.5\%$  accuracy.

### Calibration of the triaxial apparatus

The calibration of the designed triaxial apparatus was conducted before the preliminary tests on coal samples. The leakage tests were carried out to evaluate the pressure cell and gas lines, respectively. Leakage tests for the pressure cell involved testing for stability in oil pressures for a period of 1 hour using pressures at 10 MPa increments from 0-80 MPa. The results of the leakage test on pressure cell shown in fig. 2(a) confirms the stability of the pressure cell. Herein, the percentage of pressure loss over one hour for 10 MPa, 20 MPa, 30 MPa, 40 MPa, 50 MPa, 60 MPa, 70 MPa, and 80 MPa confinements are around 0.35%, 0.30%, 0.30%, 0.25%, 0.20%, 0.20%, 0.15%, and 0.10%. It means that there is no leakage observed during the tests, according to the accuracy of the pressure transducer ( $\pm 0.5\%$ ). Furthermore, the results of the axial loads for a period of 1 hour using pressures at 400 kN increments from 0 to 2 000 kN is presented in fig. 2(b), indicating that it meets requirements of the equipment.

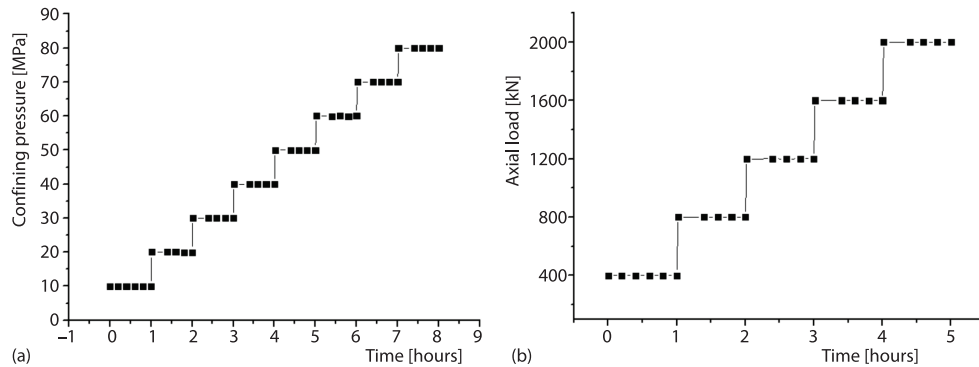


Figure 2. Results of leak tests for (a) the confining pressure and (b) the axial load

Leakage tests for the gas lines were performed using  $N_2$ . The lines were filled with  $N_2$  and held at pressure for 1 hour for each 5 MPa pressure increment between 0-25 MPa. The result for the leakage tests for the gas lines are shown in fig. 3(a). Herein, percentage of pressure loss over one hour for 5 MPa, 10 MPa, 15 MPa, 20 MPa, and 25 MPa injecting pressures are around 0.45%, 0.35%, 0.30%, 0.35%, and 0.20%. These values should represent a non-leak condition. Again, the constant pressure values can be seen from the given injection pressure, confirming that the gas lines are stable for pressures up to 25 MPa. The  $N_2$  injecting temperature is detected at temperature for 1 hour for each 30 °C temperature increment between 0-120 °C. The variation of axial pressure is less than 0.4%, fig. (3b), meets the requirements of gas injection.

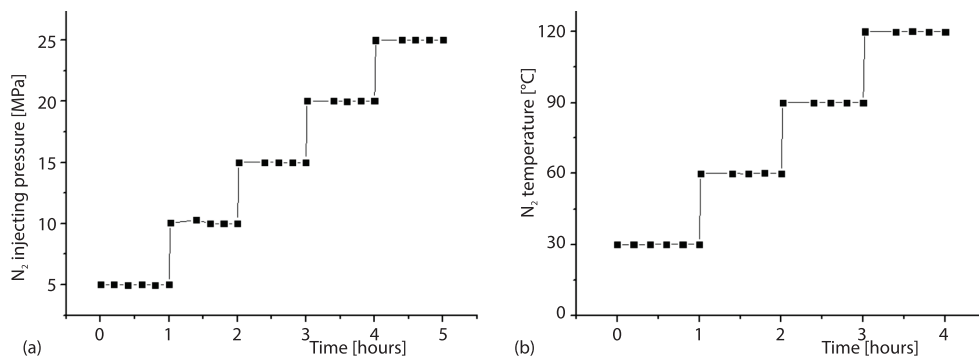


Figure 3. Results of leak tests for (a) the gas injecting pressure and (b)  $N_2$  temperature

### Verification of the experimental tests on coal samples

A series of laboratory tests were conducted to verify the feasibility of this calibrated triaxial apparatus. The coal samples were obtained from the Pingdingshan coalfield, China. The mechanical test was carried out on three coal samples under 10 MPa confining pressure, using 30 °C N<sub>2</sub> gas injection with 4 MPa, 6 MPa, and 8 MPa pressure, respectively. As listed in tab. 2, the reference sample subjected to conventional conditions was also prepared and tested for comparison. Moreover, other three coal samples under 10 MPa confining pressure using 4 MPa N<sub>2</sub> gas injection with 60 °C, 80 °C, and 100 °C were also tested. More detailed information in terms of the physical parameters and test conditions of all tested coal specimens can be found from tab. 2.

**Table 2. Physical parameters and test conditions of coal specimens**

Sample No.	Diameter [mm]	Height [mm]	Weight [g]	Confining pressure [MPa]	N <sub>2</sub> temperature [°C]	N <sub>2</sub> injecting pressure [MPa]
L-30-0	50.14	102.11	270.14	10	30	0
L-30-4	48.92	100.34	247.72	10	30	4
L-30-6	49.69	99.45	250.91	10	30	6
L-30-8	51.23	100.07	265.38	10	30	8
L-60-4	51.39	98.95	259.38	10	60	4
L-80-4	49.68	99.86	263.58	10	80	4
L-100-4	49.63	100.52	264.56	10	100	4

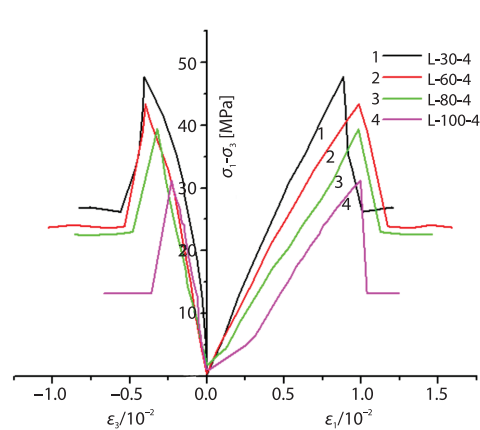


**Figure 4. Stress-strain curve of coal when N<sub>2</sub> pressure is 4 MPa**

Figure 4 presents the stress-strain curve of coal samples (where,  $\epsilon_1$  and  $\epsilon_3$  are the axial strain and circumferential strain, respectively), for which the N<sub>2</sub> injection pressure is constant. It is apparent in fig. 4 that the axial deformation of coal samples can be divided into four stages under different temperatures of N<sub>2</sub>:

- compaction stage, in which as stress increases, sample is gradually compacted, gaps in coal are gradually closed and the curve of this phase is concave down,
- elastic deformation stage, in this phase, stress and strain presents an approximate linear relationship, relationship between stress and strain accords with Hooke's law, modulus of elasticity can be regarded as a constant and it can reflect coal's ability to resist deformation,
- obedience stage, with the increasing strain, the stress increases more slowly and the stress-strain curve is more gentle as well and in this phase, cracks in sample are gradually connected and the curve presents a convex shape, and
- stage after destruction, with the increasing strain, the stress gradually drops, the sample has been destroyed and broken into several pieces, as temperature increases, triaxial compressive strength of coal decreases, the slope of elastic stage decreases, and residual strength after the destruction is gradually reduced as well.



Temperature difference exists between  $N_2$  and coal mass, heat transfer occurs between coal and  $N_2$  in its diffusion and migration process, resulting in the gradual increase of coal temperature until it the temperature difference becomes zero. Effects of  $N_2$  temperature on the deformation characteristics of the sample is mainly manifested in two aspects:

- the increase of coal's temperature changes the coal internal structure of coal matrix and
- the coal temperature's rise affects the performance of coal's adsorption towards  $N_2$ ; the higher the coal temperature is, the lower the amount of coal's adsorption towards  $N_2$  becomes and then content of free  $N_2$  increases.

Coal temperature rises so that expansive thermal stress is generated inside the sample and coal structure is destroyed, resulting in new fissures, the higher the coal temperature is, the more fissures inside the coal are, reducing coal sample's ability to resist deformation. With the increase of the content of free  $N_2$ , coal's effective stress decreases. Furthermore, when the sample is subjected to external loads, to some extent, free  $N_2$  hinders the shrinkage of fissures and promotes their extension, macroscopically, it also expresses the decrease of coal's ability to resist deformation.

Under the condition of constant temperature, the stress-strain curves of tested coal samples are depicted in fig. 5. As  $N_2$  injecting pressure increases, triaxial compressive strength of coal sample decreases, the slope of elastic stage decreases and residual strength is gradually reduced as well. Coal is to  $N_2$  what coal is to gas: for the two both, coal performs adsorption, and desorption. Although the adsorption ability of coal towards  $N_2$  is weaker than  $CH_4$ , but coal's desorption towards  $N_2$  can be done in a short time. Effects of  $N_2$  pressure on the sample is mainly reflected in two aspects. The impact of the free-state  $N_2$ . The  $N_2$  belongs to fluid, its mechanical effect (*i.e.*, fissure pressure effect) on coal sample is opposite to confining pressure's effect on coal mass. The  $N_2$  pressure can promote fissure's occurrence and development. The greater the pressure of injected  $N_2$  is, the more  $N_2$  is adsorbed in coal. Then the effective confining pressure is reduced accordingly, reducing coal sample's ability to resist external deformation forces. Therefore, gas-bearing coal's compressive strength and modulus of elasticity decrease with the increase of  $N_2$  pressure. Second is the impact of adsorbed-state  $N_2$ . For coal sample,  $N_2$  is a kind of lively fluid, generating additional impact of non-mechanical effects. After the adsorption of  $N_2$ , surface tension of fissures in coal reduces and swelling effect occurs in skeleton of coal sample, resulting in reduction of cohesion between the particles of coal sample. Consequently, the energy which is needed when destruction happens decreases, which is characterized by the decrease of compressive strength and the ability to resist deformation.

In order to analyze the mechanical properties of coal, the compressive strength, residual strength and Young's modulus of coal are calculated. The compressive strength of the coal is calculated:

$$\sigma = \sigma_1 - \sigma_3 \quad (1)$$

where  $\sigma_1$  and  $\sigma_3$  represent the axial stress and confining pressure, respectively.

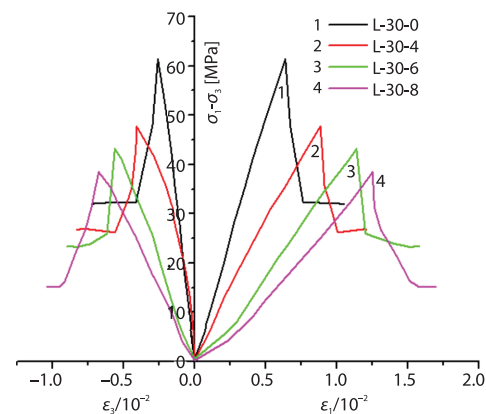


Figure 5. Stress-strain curve of coal when  $N_2$  temperature is 30 °C

The Young's modulus  $E$  can be given:

$$E = \frac{\sigma_b - \sigma_a}{\varepsilon_b - \varepsilon_a} \quad (2)$$

where  $\sigma_a$ ,  $\varepsilon_a$  are the starting point co-ordinates of the elastic stage in the stress-strain curve and  $\sigma_b$ ,  $\varepsilon_b$  – the ending point co-ordinates of the elastic stage in the stress-strain curve.

Figure 6 shows the curves of coal samples subjected to variable temperatures, in which the  $N_2$  injection pressure keeps constant (*i.e.* 4 MPa). As can be seen from fig. 6, the triaxial compressive strength of coal samples decrease with the increase of temperature. The higher temperature is, the faster the triaxial compressive strength declines. When the temperature changes, (*e.g.* 30-60 °C, 60-80 °C, and 80-100 °C), the triaxial compressive strength decreases by 0.143 MPa per °C, 0.2 MPa per °C, and 0.415 MPa per °C averagely. The residual strength of coal samples is gradually decreased with the increase of temperature. When the temperature is 30-80 °C, the residual strength is reduced slowly. Once the temperature exceeds 80 °C, the residual strength decreased quickly with the increase of temperature. It indicates that the high temperature (*i.e.* over 80 °C), the role of the internal particles is greatly weakened attributed to the thermal expansion force, reducing the residual strength of coal mass. It can be also found from fig. 6 that the Young's modulus of coal sample decreases gradually with the increase of temperature, and the decrease becomes slows. When temperature is 30-60 °C, 60-80 °C, and 80-100 °C, it decreases by 0.031 GPa per °C, 0.013 GPa per °C, and 0.012 GPa per °C, averagely.

When  $N_2$  temperature is 30 °C, the coal mechanical parameters changes with  $N_2$  injection pressure is shown in fig. 7. As illustrated in fig. 7, the triaxial compressive strength of coal, residual strength, and Young's modulus of coal sample all decrease with the increase of  $N_2$  pressure. In general, with the increase of the  $N_2$  temperature and injecting pressure, the mechanical parameters of coal sample have declined to different extents, being characterized by the decline of coal's ability to resist damage.

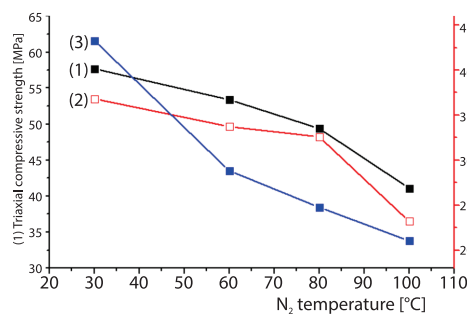


Figure 6. Mechanical parameters of coal when  $N_2$  pressure is 4 MPa

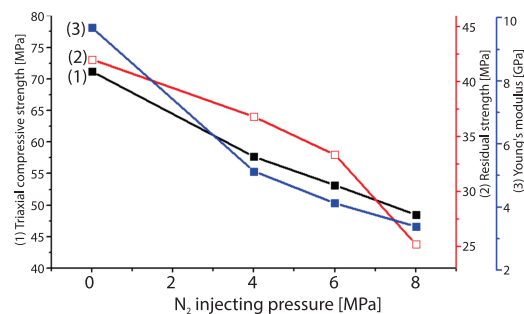


Figure 7. Condition that coal mechanical parameters when  $N_2$  temperature is 30 °C

## Conclusions

This paper introduces a new triaxial apparatus designed to study the mechanical aspects of high temperature  $N_2$  injection into coal. The new set-up consists of four main components.

- Servo loading system.
- Heating systems (for  $N_2$  or coal heating).
- Gas injection system.
- Data measurement system.



The novel aspect of this new device is gas injection with high temperature (up to 120 °C) and high pressure (up to 25 Mpa) .

A series of mechanical tests were conducted for coking coal from the Pingdingshan coalfield, China, using the new equipment. For the mechanical tests, the triaxial compressive strength, residual strength and Young's modulus decrease with the increasing of temperature and injecting pressure of N<sub>2</sub>. In other words, the higher of temperature and injecting pressure of N<sub>2</sub> are, the lower the ability to resist the destruction of coal is.

### Acknowledgment

The work presented in this paper is financially supported by the National Natural Science Foundation of China (No. 51904270 and 52078477); General Project of Philosophy and Social Science Research in Colleges and Universities in Jiangsu Province (2021SJA1120); and the Major Research Program of Natural Science of Higher Education of Jiangsu Province, China (19KJA570001).

### Nomenclature

$E$  – Young's modulus, [GPa]

Greek symbols

$\varepsilon_1$  – axial strain, [–]

$\varepsilon_3$  – circumferential strain, [–]

$\sigma$  – compressive strength, [MPa]

$\sigma_1$  – axial stress, [MPa]

$\sigma_3$  – confining pressure, [MPa]

### References

- [1] Yuan, L., Key Technique of Safe Mining in Low Permeability and Methane Rich Seam Group, *Chinese Journal of Rock Mechanics and Engineering*, 27 (2008), 6, pp. 1370-1379
- [2] Qian, M., Consideration on the Development of China Coal in Industry, *China Coal*, 31 (2005), 9, pp. 5-9
- [3] Wang, S., *et al.*, A Heat Transfer Model of High-Temperature Nitrogen Injection into a Methane Drainage Borehole, *Journal of Natural Gas Science and Engineering*, 24 (2015), 7, pp. 449-456
- [4] Zhou, F., Study on the Coexistence of Gas and Coal Spontaneous Combustion I: Disaster Mechanism, *Journal of China Coal Society*, 37 (2012), 5, pp. 843-849
- [5] He, M., *et al.*, Study on Rock Mechanics in Deep Mining Engineering, *Chinese Journal of Rock Mechanics and Engineering*, 24 (2005), 16, pp. 2803-2813
- [6] Li, M., *et al.*, Study on Deep Mining Safety Control Decision Making System, *Procedia Earth and Planetary Science*, 1 (2009), 1, pp. 377-383
- [7] Zhou, H., *et al.*, Developments in Researches on Mechanical Behaviors of Rocks under the Condition of High Ground Pressure in the Depths, *Advances in Mechanics*, 35 (2005), 1, pp. 91-99
- [8] Ranjith, P., *et al.*, A New Triaxial Apparatus to Study the Mechanical and Fluid-Flow Aspects of Carbon Dioxide Sequestration in Geological Formations, *Fuel*, 90 (2011), 3, pp. 2751-2759
- [9] Durucan, S., *et al.*, Effects of Stress and Fracture on Permeability of Coal, *Mining Science and Technology*, 3 (1986), 3, pp. 205-216
- [10] Gentzis, T., *et al.*, Geomechanical Properties and Permeability of Coals from the Foothills and Mountain Regions of Western Canada, *International Journal of Coal Geology*, 69 (2007), 3, pp. 153-164
- [11] McKee, C., *et al.*, Stress-Dependent Permeability and Porosity of Coal and Other Geologic Formations, *Spe Formation Evaluation*, 3 (1988), 1, pp. 81-91
- [12] Somerton W., *et al.*, Effect of Stress on Permeability of Coal, *International Journal of Rock Mechanics and Mining Science and Geomechanics Abstracts*, 12 (1975), 5-6, pp. 129-145
- [13] Viete, D., *et al.*, The effect of CO<sub>2</sub> on the Geomechanical and Permeability Behaviour of Brown Coal: Implications for Coal Seam CO<sub>2</sub> Sequestration, *International Journal of Coal Geology*, 66 (2006), 3, pp. 204-216
- [14] Barla, G., *et al.*, New Triaxial Apparatus for Rocks, *Rock Mechanics and Rock Engineering*, 43 (2010), 2, pp. 225-230